NJC
New Journal of Chemistry
A journal for new directions in chemistry

Accepted Manuscript

This article can be cited before page numbers have been issued, to do this please use: A. Li, C. Luo, F. WU, S. Zheng, L. Li, J. Zhang, L. Chen, K. Liu and C. Zhou, *New J. Chem.*, 2020, DOI: 10.1039/D0NJ04539J.

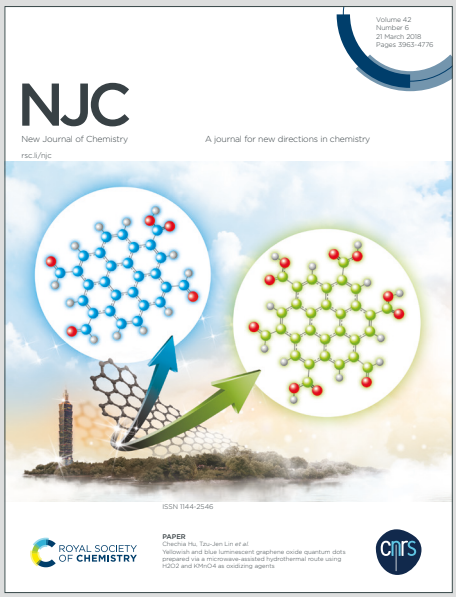

View Article Online
DOI: 10.1039/D0NJ04539J

Mesoporous HBeta Zeolite via Zeolitic Dissolution-Recrystallization Successive Treatment for Vapor-Phase Doebner-Von Miller Reaction to Quinolines

An Li [a#*], CaiWu Luo [b#], Fen Wu [a#], ShuQin Zheng [a], LiJun Li [a], JianCe Zhang [a], Liang Chen [a], Kun Liu [a*] and Congshan Zhou [a*]

[a] Province Key Laboratory for Fine Petrochemical Catalysis and Separation, College of Chemistry and Chemical Engineering, Hunan Institute of Science and Technology, Yueyang, Hunan, 414000, P. R. China.

[b] School of Environmental Protection and Safety Engineering, University of South China, Hengyang, Hunan 421001, China.

[#] Coauthors equally contributed to this work.

** Corresponding author. Email:* anleechn@hotmail.com & liukun328@126.com & zhoucongsh@126.com.

View Article Online
DOI: 10.1039/D0NJ04539J

ABSTRACT

The reassembled HBeta zeolite (HBeta-Ct) was obtained via zeolitic dissolution-recrystallization successive treatment, and characterized by means of XRD, FT-IR, SEM, TEM, N_2 adsorption-desorption as well as NH_3-TPD techniques. The characterization results manifested that the HBeta-Ct zeolite possessed more mesopores and less acid amount than the parent one. Catalyst activities of the parent and reassembled HBeta catalysts were investigated detailedly in vapor-phase Doebner-Von Miller reaction to quinolines. The results demonstrated that the reassembled HBeta zeolite showed enhanced stability of catalyst and improved ability of anti-alkylation. This is probably due to the existence of mesopores on catalyst which strengthened the diffusion of bulky products from pore channels in zeolite. Meanwhile, the decreased acid amount over catalyst can also retard the alkylation process to generate alkylquinolines as well as the acid-induced polymerization reaction to form the coking. Besides, the HBeta-Ct catalyst also exhibited good regenerability in Doebner-Von Miller reaction.

Keywords: recrystallization, Doebner-Von Miller reaction, acrolein diethyl acetal, quinolines, alkylation

View Article Online
DOI: 10.1039/D0NJ04539J

1 Introduction

Quinoline derivatives are important nitrogen-containing heterocyclic compounds used extensively in drug design.[1-3] Doebner-Von Miller reaction(DVM) is one of the most effective synthetic methods to produce quinoline derivatives.[4-9] Generally, DVM reaction employs arylamine and α, β-unsaturated aldehydes as starting materials, via michael addition of aniline and unsaturated ketone under acidic conditions and subsequent cyclization to dihydroquinoline. Although being attractive due to its straightforward workup procedures, the DVM method always is conducted via conventional liquid-phase means, which suffer from long reaction time, volatile organic solvents, complicated catalyst separation and etc.[6, 7, 10, 11] For example, Cowen et al. reported the liquid-phase DVM reaction using acrolein diethyl acetals and aniline as substrates[6]; and satisfied yield of quinoline was achieved under organic solvent conditions for 24 h with corrosive acid as catalyst. Thus, in order to avoid mentioned-above drawbacks, the further development of vapor-phase DVM reaction to quinolines is of great interest and still desirable.

Zeolites have been widely employed as heterogeneous catalysts in oil refining, gas absorption and fine chemicals, because of their high surface area, uniform pore sizes, excellent hydrothermal stability and adjustable acid sites.[12-15] Interestingly, Beta zeolite possesses more appropriate pore size (0.56×0.56 nm and 0.66×0.67 nm) to match with quinolines molecule size than the other zeolites, and it was certified to be a high-activity catalyst for the gas-phase reaction to synthesize quinolines.[16-18]. However, the property of single micropores of Beta zeolite easily imposes diffusion limitation of bulky quinolines molecule in zeolitic pore channels, thereby leading to serious catalyst deactivation. Several literatures revealed that pure microporous Beta catalyst showed low catalytic stability in the quinolines` vapor-phase synthetic reactions.[17-19] Thus, in order to overcome diffusional limitation within zeolites, creating added hierarchically pores on zeolite provides an alternative strategy to promote faster diffusion of bulky reactants and products in pore channels.

In recent years, mesoporous Beta zeolite has been widely applied in numerous bulky molecular reactions, such as, alkylation, conversion of synthesis Gas,

isomerization, benzoylation, quinolines synthesis and etc.[20-26] The catalytic evaluation results manifested that mesoporous zeolites exhibited superior catalytic activity and stability than corresponding microporous one. Mesoporous Beta zeolite could be prepared by various tactics, such as, acid/alkaline post-treatment, hard templates and soft templates method, recrystallization of amorphous zeolitic seeds or silicon aluminum source, dry-gel conversion and etc.[27-36] Among these methods, zeolitic recrystallization treatment was pursued to gain mesoporous Beta zeolite, via alkaline treatment of zeolite to form amorphous silica-alumina sources and subsequent recrystallization with template agents. Zhang et. al. reported that the Beta/MCM-41 zeolite composite could be obtained via alkali-treated zeolite and subsequent recrystallization with CTAB as template agent at alkaline environment. [30] Interestingly, Shi et al revealed that recrystallization process existed competition balance between crystallization of zeolite and self-assembly of mesoporous, and the final morphology of hierarchical materials could be regulated via adjusting the pH of crystallization system.[37] As a result, the hierarchical catalyst possessed a stepwise distributed pore structure and showed enhanced activity and sulfur tolerance in hydrogenation reaction of bulky naphthalene.[30]

Herein, in this work, the parent HBeta zeolite was improved via zeolitic dissolution-recrystallization successive treatment, and the treated HBeta zeolite (named HBeta-Ct) was used as the green solid-acid catalyst for vapor-phase Doebner-Von Miller reaction to quinolines. The activity and stability of catalysts were systematically investigated; and the relationship between texture and performance of catalysts was also discussed in this paper.

2. Experimental

2.1. Materials

All the chemicals, including acrolein dimethyl acetal, acrolein diethyl acetal, aniline, ethanol, cetyl trimethyl ammonium bromide, ammonium nitrate, acetic acid sodium hydroxide and so on, were purchased from Sinopharm Chemical Reagent Company and had analytic purity. The parent zeolites, including HY(Si/Al=6),

HUSY(Si/Al=10), HZSM-5(Si/Al=25), HBeta(Si/Al=25), were supplied by Nankai University Catalyst Factory.

2.2. Catalyst Preparation

2.2.1. Preparation of the H-formed HBeta zeolite

The H-formed Beta zeolite was treated via ion-exchange method. Firstly, the parent Beta zeolite was added into the 1.0 M NH_4NO_3 solution to reflux 4h with strong stirring at 90 °C. Afterwards, the obtained slurries were filtrated, and dried one night at 120 °C. The above processes of ion-exchange to drying were repetitively operated three times. After that, the dried solid was calcined at 550 °C for 4 h, and the thus-obtained catalyst was denoted as HBeta.

2.2.2. The treatment of HBeta zeolite via dissolution-recrystallization processes

The typical zeolitic dissolution-recrystallization successive treatment procedure, according to the previous literature,[30] is described as follows: The prepared HBeta zeolite powder was added to 1.85M solution of sodium hydroxide, and then refluxed for 70 min at 40 °C under vigorous stirring. After that, aqueous solution of cetyl trimethyl ammonium bromide (8.5g CTAB, 14.5wt%) was dropt into the above suspension under strong stirring, and the pH was adjusted to 11.1~11.3 using acetic acid. After stirring for 0.5 h, the obtained slurry was transferred into a teflon-coated stainless-steel autoclave and crystallization treated for 12-36 h at 120 °C. Then, the precipiated product was obtained via filtering, washing, dried one night at 120 °C, and calcined at 550 °C for 4 h. Finally, the catalyst was obtained through the as-above ion-exchange process and re-calcined 4 h at 550 °C. The as-prepared catalysts undergoing crystallization time for 12 h, 24 h and 36 h were named as HBeta-Ct, HBeta-Ct-24 and HBeta-Ct-36, respectively.

2.3. Catalysts Characterization

X-ray diffraction (XRD) spectra of catalysts were recorded by a Bruker D8 diffraction instrument. Operating scanning voltage was 40 kV and scanning current was 40 mA using Cu *Kα* ray (λ=1.54187 Å), scanning speed was conducted at 0.2 s and scanning step conducted at 0.02°.

Fourier transform infrared (FT-IR) spectra of catalysts were performed on a

Varian 3100 spectrometer. The sample was thoroughly mixed with KBr and then placed into sample holder to install in spectrometer cavity. Spectrums were measured using scanning number of 32 with the resolution at 2 cm^{-1}.

Scanning electron microscope (SEM) images were measured on Hitachi S4800 apparatus with accelerating voltage at 5 kV. Prior to measurement, the samples were initially adequately dispersed in ethanol, and then dropped onto the silicon chip.

Transmission electron microscope (TEM) images were tested using JEM-2100F instrument. The accelerating voltage was set at 200 kV. Before testing, samples were dispersed fully in ethanol via ultrasonic process, and doped onto the copper grid.

N_2 adsorption-desorption measurements were performed on Quantachrome Autosorb-1 instrument. The sample was firstly degassed for 12 hours with vacuum condition of 10^{-8} Torr at 300 °C, and then measured the adsorption-desorption isothermals. The multipoint BET equation analysis method was used to investigate specific surface area. The "t-plot" analysis method was employed to calculate microporous area as well as volume, and the BJH analysis methods were applied to estimate the mesopore size distribution using adsorption branch of isotherms.

Temperature-programmed desorption of ammonia (NH_3-TPD) was performed on Autochem II 2920 apparatus. Before NH_3 adsorption, the samples were treated at 400 °C in the flow of He (60ml/min) for 0.5 h. Later on, the sample began to adsorb NH_3 up to saturation with 10 vol.% NH_3 in the flow of He (50 ml/min). Then, physically adsorbed NH_3 was thoroughly purged for 1 using He flow at 100 °C. Finally, ammonia on sample was desorbed in the range 100~800 °C with 10 °C/min heating rates.

Thermogravimetry (TG) measurements were performed on Diamond apparatus. The deactivated catalysts were heated from 25 °C to 800 °C in a flow of air (30 mL/min) under 5 °C/min heating rates.

2.4. Catalytic Performance Evaluation

Vapor-phase Doebner-Von Miller reaction was performed in the fixed-bed reactor, and the typical operating process was as follows: firstly, 1.0g of catalyst was

placed in the middle of the stainless steel reaction tuber (*i.d.* 8mm), and then heated in nitrogen flow of 30mL/min until reaching reaction temperature. Subsequently, the feedstocks mixtures, containing aniline(AN) and acrolein acetal(AA), were fed into the fixed-bed reactor. The products were collected and cooled using ice-water trap. The product mixtures were analyzed and identified on Varian Saturn 2200/CP-3800 gas chromatography-mass spectrometry, in which two CP8944 capillary columns (VF-5, 30m×0.25mm×0.25μm) were equipped and connected to flame ionization detector and mass detector. The yield of quinoline(Q), methylquinoline(MeQ) and ethylquinoline(EtQ) were calculated based on the converted acrolein acetal(AA).

$$Conversion\ (mol\%) = \frac{moles\ of\ AA\ converted}{moles\ of\ AA\ input} \times \%$$

$$Selectivity\ (mol\%) = \frac{moles\ of\ product}{moles\ of\ AA\ converted} \times \%$$

$$Yield\ (mol\%) = Conversion \times Selectivity \times \%$$

3. Results and Discussions

3.1. Catalyst Characterization

The XRD patterns of catalysts are shown in figure 1(*a*). After crystallization for 12 h, the framework structure of HBeta zeolite is well generated. Interestingly, mordenite phase begin to form in zeolite after recrystallization to 24 h, and more mordenite phase as well as other additional phase generate in zeolite as further prolonging crystallization time to 36 h. Several literatures reported that post-synthesis treatments could induce formation of additional phases.[35, 38] It infers that mordenite phase and other additional phase could be generated from zeolitic fragments as prolonging recrystallization time. Obviously, the intensity of peaks over HBeta-Ct decrease than that over HBeta, owing to the decreased relative crystallinity (94.3%) of HBeta-Ct (table 1S). The small-angle XRD pattern of HBeta-Ct shows no obvious peak (figure 1S). it indicates that the ordered mesoporous MCM-41 phase was not formed during the CTAB&NaOH co-treatment process. In addition, the ratio of Si/Al ratio of HBeta-Ct decreases slightly. This is probably due that some silicon species

dissolved in alkali solution and was not assembled to rebuild framework of zeolite. As a result, 93.4% yield of product is obtained.

Generally, alkaline post-treatment could generate mesopores within zeolite and also retain main the structure of zeolite, via extracting silicon from framework of zeolite. The XRD patterns of alkali-treated parent HBeta zeolites with different alkali concentration are shown in figure 2S. Clearly, parent HBeta zeolites retain partly framework structure using low-concentration alkali treatment (<0.6 mol/L), while parent HBeta zeolites structure is destroyed entirely to form amorphous phase at high-concentration alkali treatment under the same operation condition (> 1.0 mol/L). this shows that the zeolite structure of HBeta-Ct is not from the retained parent structure of HBeta zeolite through high-concentration alkali treatment. It infers that the formed amorphous phases consist of zeolitic fragments and even zeolite seeds,[38] which favors the following zeolitic reassembling process. It indicates that the forming zeolite structure of HBeta-Ct is ascribed to the reassembling of amorphous phase.

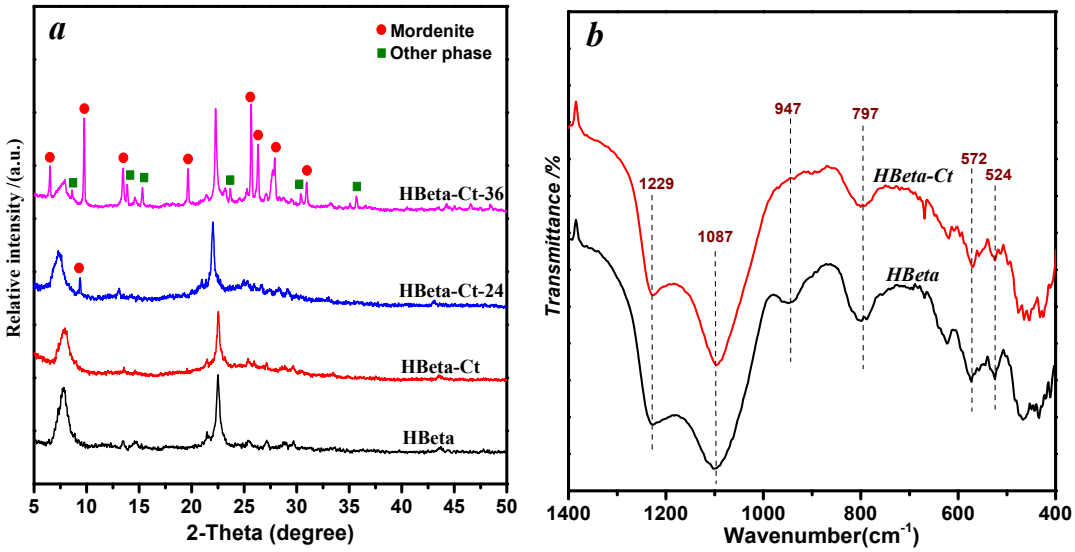

Figure 1. the XRD patterns(*a*) and FT-IR spectra(*b*) for catalysts

The FT-IR spectras of catalysts are shown in figure 1(*b*). The bands at ca. 797, 1087, and 1229 cm^{-1} are related to the external symmetric, internal asymmetric and external asymmetric stretching vibrations of tetrahedron units, respectively.[39-41] Moreover, the bands at ca. 524 and 568 cm^{-1} are presumably attributed to framework

characteristic of Beta zeolite.[42, 43] Obviously, HBeta-Ct zeolite shows good characteristic vibrations of Beta zeolite, while the bands intensities of HBeta-Ct zeolite decrease slightly relative to the parent HBeta one. The results further demonstrate that HBeta-Ct zeolite possesses a good zeolite framework structure but its crystallinity reduces accordingly.

The HRTEM micrographs of catalysts are shown in figure 2. The parent HBeta zeolite is free of intracrystalline defects and shows a clear crystal lattice in the framework. This indicates the high crystallinity of parent HBeta zeolite.[44] However, the HBeta-Ct zeolite presents obvious defects liking irregular cracks. This may be relating to the generation of mesopores, thereby forming the hierarchical structure.[34] In addition, as shown in SEM micrographs (see in figure 3S), the parent HBeta zeolite consists of many bulk irregular agglomerate crystal grains, but the HBeta-Ct zeolite shows larger size of crystal grains than the parent HBeta one.

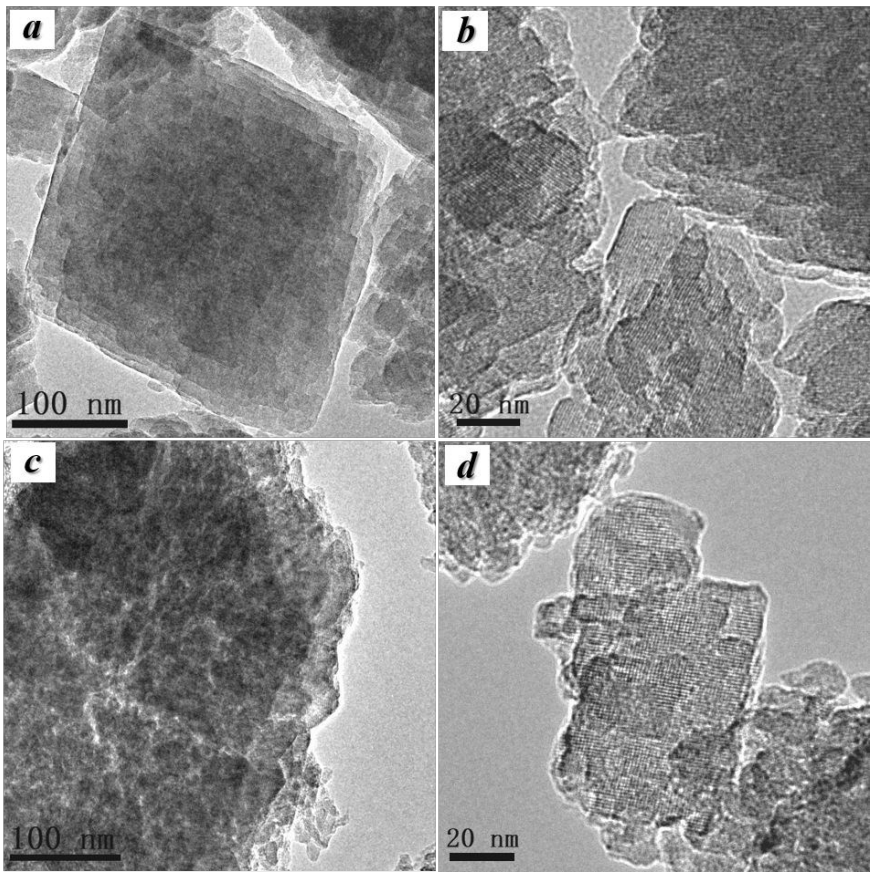

Figure 2. The TEM images of HBeta(*a, b*) and HBeta-Ct(*c, d*)

The N_2 adsorption-desorption isotherms of catalysts are shown in figure 3(*a*). The isotherms rise rapidly at low relative pressure over all catalysts, due to the adsorption of N_2 in micropore. A prominent hysteresis loop is present over the HBeta-Ct zeolite but absent over the parent HBeta one at P/P_0>0.4. The appearance of hysteresis loop further indicates the existence of certain mesopores over HBeta-Ct zeolite. The specific textural properties of the catalysts are listed detailedly in table 1. The S_{mic}, S_{ext}, S_{BET} as well as V_{mic} over the HBeta-Ct zeolite decreases to some extent, compared to the parent HBeta one. Interestingly, the HBeta-Ct zeolite possesses as high as 0.61mL/g of mesopore volume, and mesopore size is centered at ca. 3.85 nm. The result illustrates that zeolitic dissolution-recrystallization successive treatment generates mesopores approvingly.

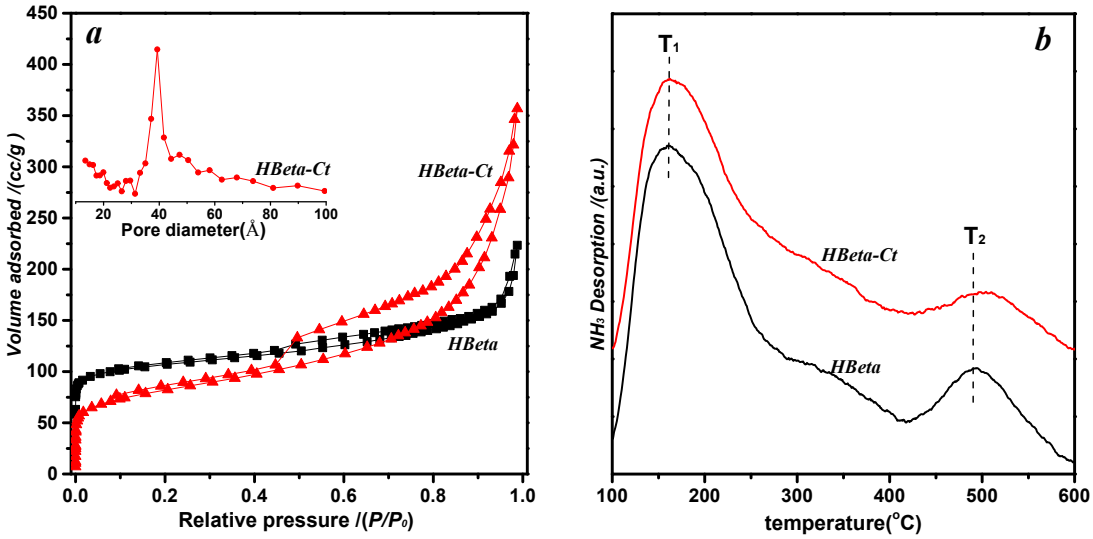

Figure 3. the N_2 absorption-desorption isotherms(*a*) and NH_3-TPD(*b*) for catalysts

Table 1. the textural properties of catalysts.

Catalyst	S_{BET} (m^2/g)	S_{ext} (m^2/g)	S_{mic} (m^2/g)	V_{total} (cm^3/g)	V_{mic} (cm^3/g)	V_{meso} (cm^3/g)	D_{meso} (nm)
HBeta	483.7	168.2	315.5	0.40	0.15	0.25	-
HBeta-Ct	332.4	99.1	233.2	0.72	0.11	0.61	3.85

S_{BET}, S_{ext} and S_{mic} refers to specific surface area, external surface area and micropore surface area, respectively, and $S_{BET} = S_{ext} + S_{mic}$; Vt_{total} and V_{mic} refers to total pore volume and micropore volume, respectively; D_{meso} refers to mesopore size calculated by the BJH method.

The NH_3-TPD profiles of catalysts are exhibited in figure 3(*b*), and the detail acidity data are summarized in table 2. Both of zeolites present two desorption peaks

evidently in the range 100~200 °C and 450~550 °C. The low-temperature peak is generally belonging to weak acid sites. The high-temperature peak is responsible for strong acid sites. Generally, weak acid sites over zeolite are generally associated to terminal acid silanol groups of zeolite,[45, 46] and strong acid sites are assigned to bridging Si-(OH)-Al group of zeolite. The HBeta-Ct zeolite presents smaller low-temperature as well as high-temperature peaks than the parent HBeta one. The result indicates that both weak and strong acid sites decrease slightly over the HBeta-Ct zeolite, as shown in table 2.

Table 2. the NH_3-TPD results for catalysts.

Catalyst	T_i[a] (°C) and A_i[b] (mmol/g) for various desorption peaks					
	T_1	A_1	T_2	A_2	A_{total}	A_2/A_1
HBeta	159.6	1.23	494.5	0.35	1.58	0.28
HBeta-Ct		0.86		0.19	1.05	0.22

[a] T_i refers to the temperature at the maximum of desorption peak i.

[b] A_i refers to the integral area of desorption peak i, and it means also the concentration of acid site corresponding to the desorption peak i; A_{total} stands for the sum of the concentration of various acid site, i.e., $A_{total} = \sum Ai$.

Therefore, the above results demonstrate that, relative to the parent HBeta zeolite, the reassembled HBeta zeolite via zeolitic dissolution-recrystallization processes possesses more mesopores and less concentration of weak and strong acid sites.

3.2 Catalytic Activity

Vapor-phase Doebner-Von Miller reaction to quinolines is conducted in fixed-bed reactor, utilizing aniline and acrolein acetals as starting materials. Firstly, two types of acrolein acetals are employed as feedstock to synthesize quinolines over the parent HBeta catalyst. As shown in figure 4(*a*). The experiments results exhibit that both acrolein dimethyl acetal(AMA) and acrolein diethyl acetal(ADA) are converted with 100% at high temperature. The products of Q, MeQ and EtQ are generated distinctly in this reaction. According to previous literatures, it infers that Q, MeQ and EtQ are generated with ADA as reactant via different paths. As shown in Eq.(1-5), ADA is firstly hydrolyzed to acrolein and ethanol (Eq. 1). Then, aniline reacts with acrolein to yield Q via Michael addition-aromatization processes (Eq. 2).[47]

Quinoline can further react with ethanol to produce EtQ via alkylation over acid sites.[48] Meanwhile, ADA and acrolein can be cracked to generate acetaldehyde over solid-acid catalyst at high temperature (Eq. 4).[49] The generated acetaldehyde could react with aniline to yield MeQ (Eq. 5).[16] Apparently, total yields of Q_s (containing Q, MeQ and EtQ) increases up to ca. 76% from ca. 60.8% using ADA as feedstock, compared to AMA using in this reaction. Thus, ADA is utilized as preferred feedstock in this reaction.

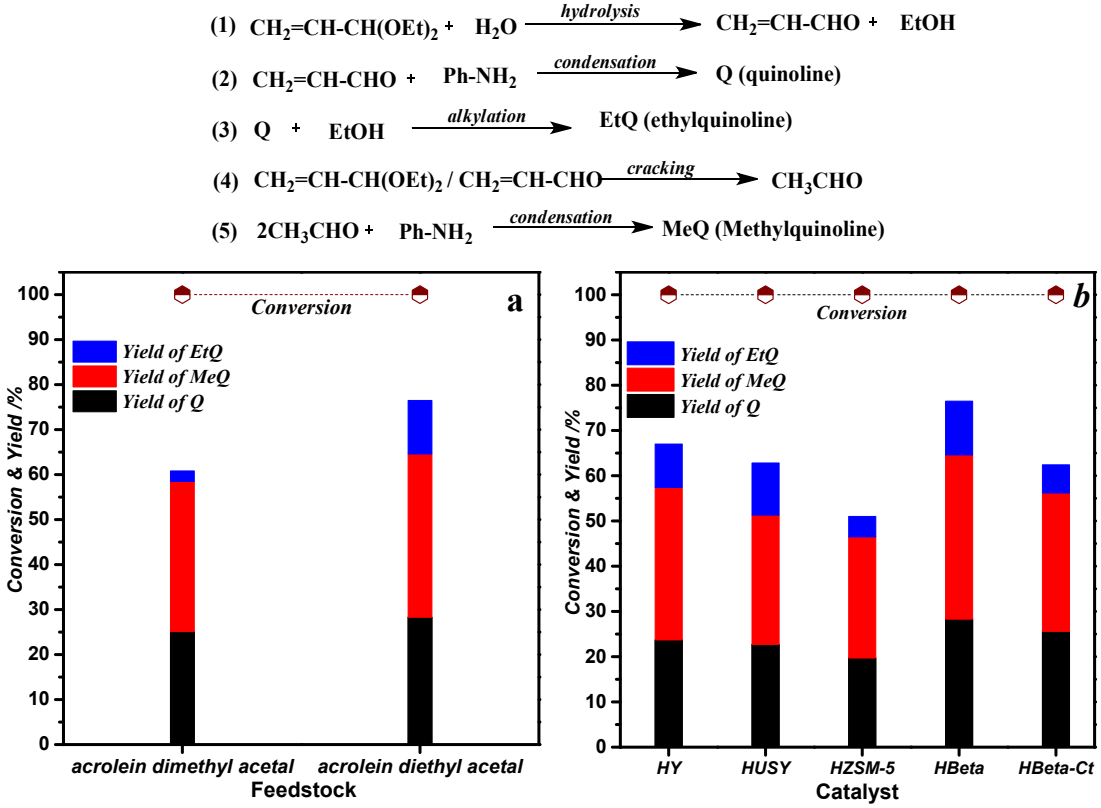

Figure 4. the effect of feedstocks(***a***) and various zeolite catalysts(***b***)
Reaction condition: temperature(440 °C), ratio of AN/ADA(3:1), LHSV of mixture feedstocks(1.0 h^{-1}), LHSV of H_2O(1.0 h^{-1}), reaction time(1 h). Q, MeQ and EtQ refer respectively to quinoline, methylquinoline and ethylquinoline.

As comparison, catalytic activities of different types of zeolites are also tested, and the catalytic results are shown in figure 4(*b*). The total yields of Q_s obtained over catalysts show an order of HBeta > HY > HUSY > HZSM-5. Interestingly, this sequence of the yield of Q_s is not consistent with the total acid amount over zeolite (see figure 4S and table 2S). It infers that the catalytic activities are influenced by not only acid amount but also porous structure of zeolite. For instance, ZSM-5 zeolite

may impose diffusion limitation of bulky products because of its small intersected pore (0.53×0.56 nm and 0.51×0.55 nm). Both of HY and HUSY zeolites could lead to deep polymerization of products due to its supercages structure. While Beta zeolite possesses large micropore channel (0.56×0.56 nm and 0.66×0.67 nm), which matches well with quinolines molecule size. Thus, both of the acidity and porous structure are responsible for the catalytic activity over various zeolites. Besides, the yield of Q, MeQ and EtQ decreases slightly over HBeta-Ct catalyst, relative to the parent HBeta one. Due to acid sites acting as the effective activity sites in DVM reaction to generate quinolines, the decrease of acid amount over HBeta-Ct reduces the yield of Q_s.

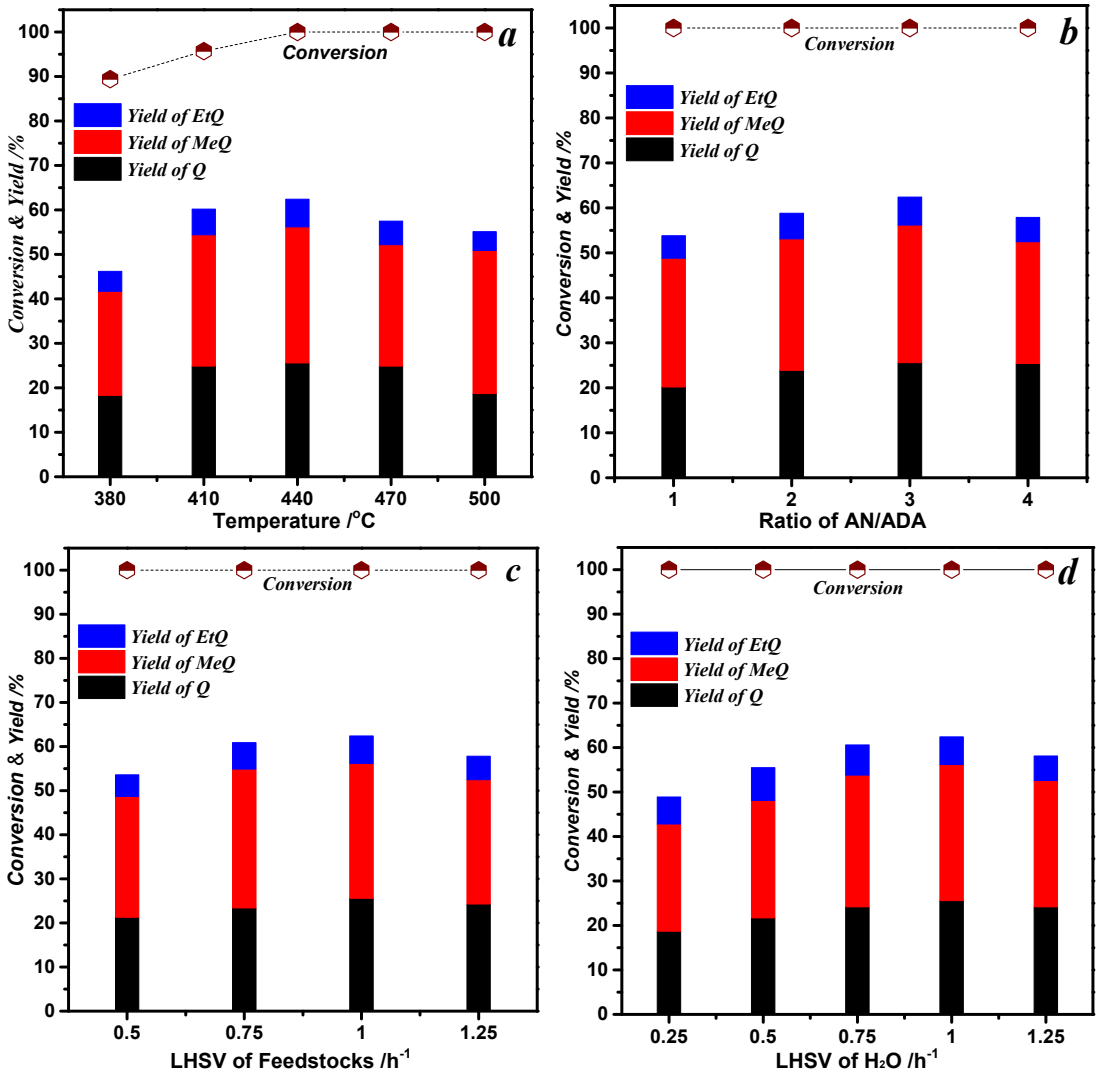

Figure 5. the effect of reaction conditions over the HBeta-Ct catalyst

Reaction condition: Temperature(*a*): ratio of AN/ADA(3:1), LHSV of mixture feedstocks(1.0 h^{-1}), LHSV of H_2O(1.0 h^{-1}). Ratio of AN/ADA(*b*): temperature(440 °C), LHSV of mixture feedstocks(1.0 h^{-1}), LHSV of H_2O(1.0 h^{-1}). LHSV of mixture feedstocks(*c*): temperature(440 °C),

ratio of AN/ADA(3:1), LHSV of H_2O(1.0 h^{-1}). LHSV of H_2O(*d*): temperature(440 °C), ratio of AN/ADA(3:1), LHSV of mixture feedstocks(1.0 h^{-1}).

Reaction influence factors are systematically investigated over HBeta-Ct zeolite. The effect of temperature is shown in figure 5(*a*). Total yields of Q_s are just ca. 55% at 380 °C. With elevating temperature, the total yields increase sharply, arriving to ca. 76% at 440 °C as its maximum, and then decreases obviously. Generally, relatively high temperature favors vapor-phase synthesis of quinolines.[17] Whereas exceeding 450 °C leads to excessive cracking of ADA and polymerization of active intermedium, thereby decreasing yield of quinolines.

The effect of the ratio of AN/ADA is shown in figure 5(*b*). Yield of Q_s and Q increases clearly as increasing AN/ADA ratio, and reaches to its optimum value at AN/ADA ratio of 3. Generally, elevating ratio of AN/ADA could increase contact opportunity of reactants, promoting the generation of quinolines. However, too high ratio of AN/ADA gives rise to alkalescent aniline excessively occupying acid sites of catalyst, which is bad for reaction process.

The effect of LHSV of mixture feedstocks is shown in figure 5(*c*). obviously, yield of Q_s and Q achieve the highest values at LHSV of 1.0 h^{-1}. Generally, reducing the LHSV could increase stay time of reactants over catalyst, thereby affecting the degree of reaction. The reaction is conducted more completely as prolonging stay time of reactants on the catalyst. Nevertheless, the probability of side reactions, such as, acrolein polymerization and coking forming, increases with further prolonging long staying time.

The effect of LHSV of H_2O is shown in figure 5(*d*). Obviously, the highest yield of Q_s as well as Q is obtained at H_2O LHSV of 1.0 h^{-1}. In fact, addition of H_2O into reactor has notable influence on yield of Q and Q_s. Because H_2O feeding into reaction system not only facilitates hydrolysis of ADA but also retards acrolein polymerization and/or other side-reactions via diluting concentration of active intermediate.

Catalyst life of the parent and reassembled HBeta zeolite catalysts are also evaluated. As the increasing of reaction time, the yield of Q and Q_s decreases to varying degrees over both of catalysts (figure 6*a*). Compared to the parent HBeta

catalyst, deactivation rate becomes slower distinctly over the HBeta-Ct one (figure 6*a*). For instance, as prolonging reaction time to 12 hours, only 28% of relative catalytic activity is reserved over the parent HBeta catalyst, whereas more than 74% of relative catalytic activity is remained over the HBeta-Ct one (figure 7*b*). Therefore, the result demonstrates that the HBeta-Ct catalyst exhibits stronger ability to inhibit deactivation than the parent HBeta one. On one hand, the existence of mesoporous over HBeta-Ct zeolite reduces diffusional limitation of bulky products. On the other hand, the decreasing of acid amount (especially strong acid sites) over HBeta-Ct zeolite restrains the acid-induced polymerization side reactions. As a result, the HBeta-Ct catalyst could accelerate the leaving of products (liking quinolines) from pore channels in zeolite and restrict the formation and deposition of the coking in pore channels of catalyst.

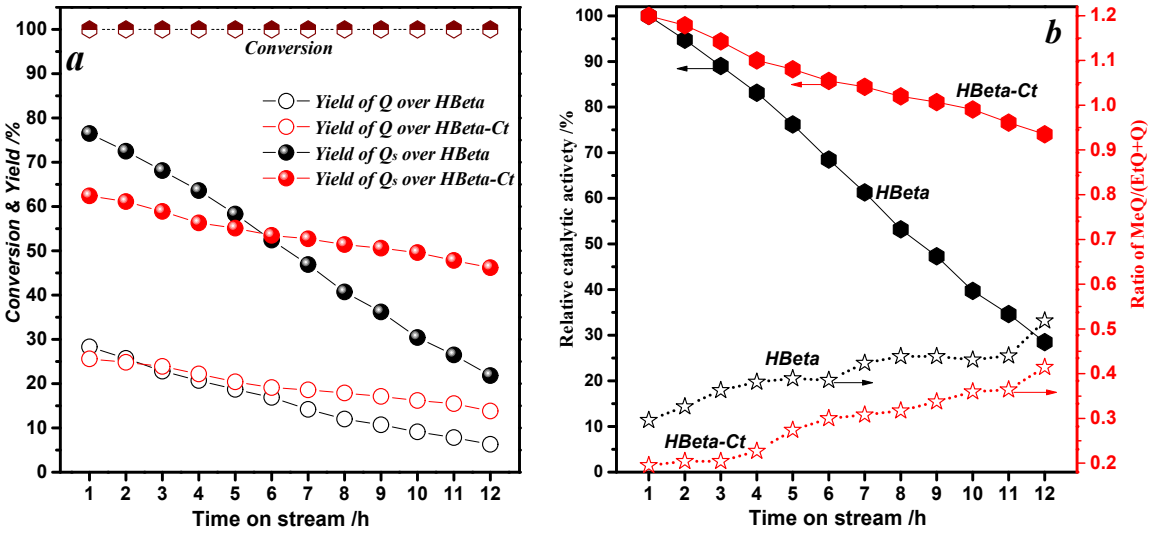

Figure 6. catalyst life of the HBeta and HBeta-Ct catalysts

Reaction condition: temperature(440 °C), ratio of AN/ADA(3:1), LHSV of mixture feedstocks(1.0 h^{-1}), LHSV of H_2O(1.0 h^{-1}). Relative catalytic activity was estimated via the yield of $Q_{s(\text{different time})}$ divided that of $Q_{s(\text{the first hour})}$)

On the basis of EtQ generating from alkylation of Q with ethanol, as shown in Eq.(1-5), the ratio value of EtQ/(EtQ+Q) could be considered to reflect alkylation degree of Q to EtQ; i.e. the smaller the ratio value, the lower the alkylation degree. Obviously, the ratio value of EtQ/(EtQ+Q) over HBeta-Ct is lower than that over HBeta at each same time nodes (figure 6*b*). It indicates that the HBeta-Ct catalyst sharply retards alkylation process, which exhibits better ability of anti-alkylation than

the HBeta one. This is possibly due to more mesopores as well as lower acid sites amount over HBeta-Ct zeolite than that over the HBeta one. Because the existence of mesoporous strengthen the diffusion of Q from the internal of catalysts and then decrease the probability of alkylation of Q with ethanol. Meanwhile, the lower acid amount over HBeta-Ct could also decrease the alkylation processes. Besides, this ratio value of EtQ/(EtQ+Q) rises obviously over both of catalyst, as prolonging reaction time (figure 6*b*). This shows that, with the increasing of reaction time, the alkylation increases clearly. Therefore, the result indicates that the HBeta-Ct catalyst could not only enhance the stability of catalyst significantly but also restrict the alkylation process distinctly.

The regenerability of the HBeta and HBeta-Ct catalysts is shown in figure 7. Apparently, catalytic activities of the deactivated HBeta and HBeta-Ct catalysts are resumed almost completely, after calcining straightforwardly at 550 C in air for 4 h. It suggests that both of catalyst exhibits a good regenerability. The deactivation is possible due to the deposition of coking on internal surface of catalyst. Because the coking on catalysts can be easily removed via calcining at 550 C in air for 4 h, and catalytic activity of both catalysts are almost fully recovered. In addition, the thermogravimetric measurements of deactivated catalysts are shown in figure 4S. The loss of weight at 345~700 °C should arise from the combustion of the coking. Obviously, the HBeta-Ct zeolite catalyst shows lower loss rate of weight, indicating stronger ability of anti-coking in DVM reaction.

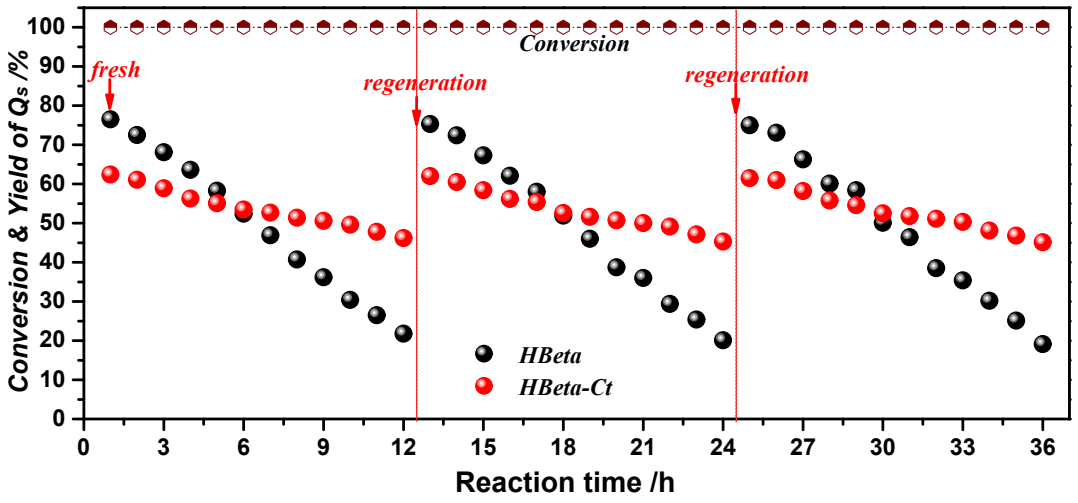

View Article Online
DOI: 10.1039/D0NJ04539J

Figure 7. the regenerability of the HBeta and HBeta-Ct catalysts

Reaction condition: temperature(440 ^{o}C), ratio of AN/ADA(3:1), LHSV of mixture feedstocks(1.0 h^{-1}), LHSV of H_2O(1.0 h^{-1}). The deactivated catalysts were regenerated via calcining at 550 ^{o}C in air for 4 h.

4. Conclusions

Mesoporous HBeta-Ct zeolite was prepared by means of zeolitic dissolution-recrystallization successive processes, and used as the green and efficient solid-acid catalyst for vapor-phase Doebner-Von Miller reaction to quinolines. The HBeta-Ct zeolite possessed more mesopores but less acidic concentration, which exhibited higher selectivity of Q, better ability of anti-alkylation and enhanced stability of catalyst, relative to the HBeta one. This is presumably due to the existence of mesopores as well as the decrease of strong acid sites over the HBeta-Ct zeolite, which could improve diffusion limitation of products, decrease the alkylation of Q as well as retard deposition of the coking. Besides, the HBeta-Ct catalysts also exhibited good regenerability in Doebner-Von Miller reaction.

Acknowledgments

This work was supported by the National Natural Science Foundation of China (No. 51978648 and 51804116), the Hunan Provincial Natural Science Foundation of China (No. 2019JJ50215).

References

[1] M. Ramanathan, J. Wan, Y.-H. Liu, S.-M. Peng and S.-T. Liu, *Org. Biomol. Chem.*, 2020, **18**, 975-982.
[2] J. Xu, Q. Chen, Z. Luo, X. Tang and J. Zhao, *RSC Adv.*, 2019, **9**, 28764-28767.
[3] L. Yang and J.-P. Wan, *Green Chem.*, 2020, **22**, 3074-3078.
[4] C. M. Leir, *J. Org. Chem.*, 1977, **42**, 911-913.
[5] Y. Kobayashi, J. Igarashi, C. Feng, Toshifumi and Tojo, *Tetrahedron Lett.*, 2012, **53**, 3742-3745.
[6] G. A. Ramann and B. J. Cowen, *Tetrahedron Lett.*, 2015, **56**, 6436-6439.
[7] A. Carral-Menoyo, N. Sotomayor and E. Lete, *Catal. Sci. Technol.*, 2020, **10**, 5345-5361.
[8] A. Das, N. Anbu, P. Varalakshmi, A. Dhakshinamoorthy and S. Biswas, *New J. Chem.*, 2020, **44**, 10982-10988.
[9] H. Vuong, M. R. Stentzel and D. A. Klumpp, *Tetrahedron Lett.*, 2020, **61**, 151630.

[10] X. Zhou, Z. Qi, S. Yu, L. Kong, Y. Li, W.-F. Tian and X. Li, *Adv. Synth. Catal.*, 2017, **359**, 1620-1625.
[11] G. S. Kumar, P. Kumar and M. Kapur, *Org. Lett.*, 2017, **19**, 2494-2497.
[12] A. B. Halgeri and J. Das, *Appl. Catal., A*, 1999, **181**, 347-354.
[13] N. Katada, Y. Kageyama, K. Takahara, T. Kanai, H. Ara Begum and M. Niwa, *J. Mol. Catal. A: Chem.*, 2004, **211**, 119-130.
[14] D. H. Choo, H. J. Kim, B. H. Kong, I. S. Choi, Y. C. Ko, H. C. Lee, J. C. Kim and J. S. Lee, *J. Catal.*, 2002, **207**, 183-193.
[15] K. Hensen, C. Mahaim and W. F. HiSlderich, *Appl. Catal., A*, 1997, **149**, 311-329
[16] R. Brosius, D. Gammon, F. Vanlaar, E. Vansteen, B. Sels and P. Jacobs, *J. Catal.*, 2006, **239**, 362-368.
[17] A. Li, C. Huang, C. W. Luo, W. J. Yi and Z. S. Chao, *RSC Adv.*, 2017, **7**, 9551-9561.
[18] A. Li, C. Huang, C.-W. Luo, L.-J. Li, W.-J. Yi, T.-W. Liu and Z.-S. Chao, *Catal. Commun.*, 2017, **98**, 13-16.
[19] A. Li, C. Luo, Y. Liu, L. Li, Y. Lin, K. Liu and C. Zhou, *Molecular Catalysis*, 2020, **486**, 110833.
[20] J. Jin, X. Ye, Y. Li, Y. Wang, L. Li, J. Gu, W. Zhao and J. Shi, *Dalton Trans.*, 2014, **43**, 8196-8204.
[21] C. Yin, D. Tian, M. Xu, Y. Wei, X. Bao, Y. Chen and F. Wang, *J. Colloid Interf. Sci*, 2013, **397**, 108-113.
[22] F. Tian, Y. Wu, Q. Shen, X. Li, Y. Chen and C. Meng, *Microporous Mesoporous Mater.*, 2013, **173**, 129-138.
[23] Y. Wu, F. Tian, J. Liu, D. Song, C. Jia and Y. Chen, *Microporous Mesoporous Mater.*, 2012, **162**, 168-174.
[24] F. Tian, X. Yang, Y. Shi, C. Jia and Y. Chen, *J. Nat. Gas Chem.*, 2012, **21**, 647-652.
[25] K. Cheng, J. Kang, S. Huang, Z. You, Q. Zhang, J. Ding, W. Hua, Y. Lou, W. Deng and Y. Wang, *ACS Catal.*, 2012, **2**, 441-449.
[26] H. Yang, Z. Liu, H. Gao and Z. Xie, *Appl. Catal., A*, 2010, **379**, 166-171.
[27] J. Zhu, Y. Zhu, L. Zhu, M. Rigutto, A. van der Made, C. Yang, S. Pan, L. Wang, L. Zhu, Y. Jin, Q. Sun, Q. Wu, X. Meng, D. Zhang, Y. Han, J. Li, Y. Chu, A. Zheng, S. Qiu, X. Zheng and F. S. Xiao, *J. Am. Chem. Soc.*, 2014, **136**, 2503-2510.
[28] A. Ishihara, K. Inui, T. Hashimoto and H. Nasu, *J. Catal.*, 2012, **295**, 81-90.
[29] K. Moller, B. Yilmaz, R. M. Jacubinas, U. Muller and T. Bein, *J Am Chem Soc*, 2011, **133**, 5284-5295.
[30] H. Zhang and Y. Li, *Powder Technol.*, 2008, **183**, 73-78.
[31] Y. Tong, T. Zhao, F. Li and Y. Wang, *Chem. Mater.*, 2006, **18**, 4218-4220.
[32] S. Bernasconi, J. A. van Bokhoven, F. Krumeich, G. D. Pirngruber and R. Prins, *Microporous Mesoporous Mater.*, 2003, **66**, 21-26.
[33] W. Guo, C. Xiong, L. Huang and Q. Li, *J. Mater. Chem.*, 2001, **11**, 1886-1890.
[34] N. Suárez, J. Pérez-Pariente, F. Mondragón and A. Moreno, *Microporous Mesoporous Mater.*, 2019, **280**, 144-150.
[35] K. Zhang, S. Fernandez, S. Kobaslija, T. Pilyugina, J. O'Brien, J. A. Lawrence and M. L. Ostraat, *Ind. Eng. Chem. Res.*, 2016, **55**, 8567-8575.
[36] A. Karlsson, M. Stöcker and R. Schmidt, *Microporous Mesoporous Mater.*, 1999, **27**, 181-192.
[37] H. Li, H. Wu and J.-l. Shi, *J. Alloy. Compd.*, 2013, **556**, 71-78.
[38] I. I. Ivanova and E. E. Knyazeva, *Chem. Soc. Rev.*, 2013, **42**, 3671-3688.
[39] A. Vimont, F. Thibault-Starzyk and J. C. Lavalley, *J. Phys. Chem. B*, 2000, **104**, 286-291.

[40] I. Othman, R. M. Mohamed, I. A. Ibrahim and M. M. Mohamed, *Appl. Catal., A*, 2006, **299**, 95-102.

[41] L. Shirazi, E. Jamshidi and M. R. Ghasemi, *Cryst. Res. Technol.*, 2008, **43**, 1300-1306.

[42] J. Perez-Pariente, J. A. Martens and P. A. Jacobs, *Appl. Catal.*, 1987, **31**, 35-64.

[43] I. Kiricsi, C. Flego, G. Pazzuconi, W. O. Parker, Jr., R. Millini, C. Perego and G. Bellussi, *J. Phys. Chem.*, 1994, **98**, 4627-4634.

[44] H. Yang, P. Yang, X. Liu and Y. Wang, *Chem. Eng. J.*, 2016, **299**, 112-119.

[45] Y. T. Kim, K. D. Jung and E. D. Park, *Microporous Mesoporous Mater.*, 2010, **131**, 28-36.

[46] B. O. D. Costa, M. A. Peralta and C. A. Querini, *Appl. Catal., A*, 2014, **472**, 53-63.

[47] B. M. Reddy and I. Ganesh, *J. Mol. Catal. A: Chem.*, 2000, **151**, 289-293.

[48] P. R. Reddy, K. V. S. Rao and M. Subrahmanyam, *Catal. Lett.*, 1998, **56**, 155-158.

[49] L. Shen, H. Yin, A. Wang, Y. Feng, Y. Shen, Z. Wu and T. Jiang, *Chem. Eng. J.*, 2012, **180**, 277-283.

View Article Online
DOI: 10.1039/D0NJ04539J

Graphical Abstract

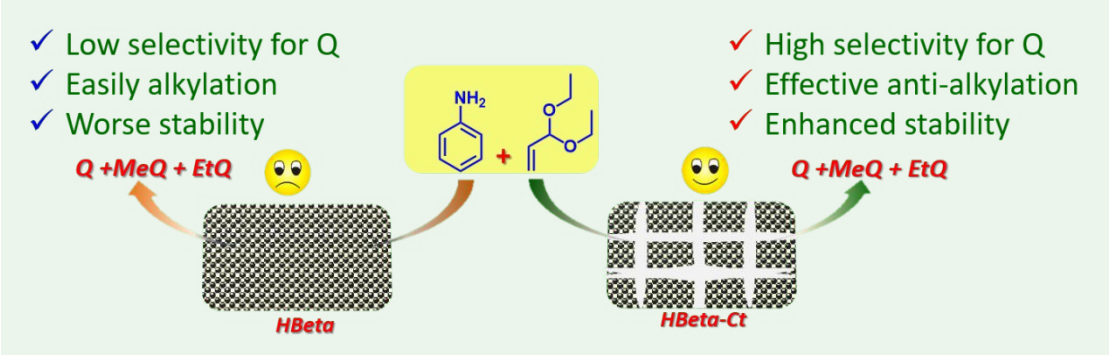

Mesoporous HBeta zeolite was obtained via zeolitic dissolution-recrystallization successive treatment, which exhibited higher selectivity of Q, better ability of anti-alkylation as well as catalyst stability in vapor-phase Doebner-Von Miller reaction, relative to the HBeta one.